

# Ca<sup>2+</sup> signals mediated by Ins(1,4,5)P<sub>3</sub>-gated channels in rat ureteric myocytes

François-Xavier BOITTIN, Frédéric COUSSIN, Jean-Luc MOREL, Guillaume HALET, Nathalie MACREZ and Jean MIRONNEAU<sup>1</sup>

Laboratoire de Physiologie Cellulaire et Pharmacologie Moléculaire, CNRS UMR 5017, Université de Bordeaux II, 146 rue Léo Saignat, 33076 Bordeaux Cedex, France

Localized Ca<sup>2+</sup>-release signals (puffs) and propagated Ca<sup>2+</sup> waves were characterized in rat ureteric myocytes by confocal microscopy. Ca<sup>2+</sup> puffs were evoked by photorelease of low concentrations of Ins(1,4,5)P<sub>3</sub> from a caged precursor and by low concentrations of acetylcholine; they were also observed spontaneously in Ca<sup>2+</sup>-overloaded myocytes. Ca<sup>2+</sup> puffs showed some variability in amplitude, time course and spatial spread, suggesting that Ins(1,4,5)P<sub>3</sub>-gated channels exist in clusters containing variable numbers of channels and that within these clusters a variable number of channels can be recruited. Immunodetection of Ins(1,4,5)P<sub>3</sub> receptors revealed the existence of several spots of fluorescence in the confocal cell sections, supporting the existence of clusters of Ins(1,4,5)P<sub>3</sub> receptors. Strong Ins(1,4,5)P<sub>3</sub> photorelease and high concentrations of acetylcholine induced Ca<sup>2+</sup> waves that originated from an initiation site and propagated in the whole cell by spatial recruitment of

neighbouring Ca<sup>2+</sup>-release sites. Both Ca<sup>2+</sup> puffs and Ca<sup>2+</sup> waves were blocked selectively by intracellular applications of heparin and an anti-Ins(1,4,5)P<sub>3</sub>-receptor antibody, but were unaffected by ryanodine and intracellular application of an anti-ryanodine receptor antibody. mRNAs encoding for the three subtypes of Ins(1,4,5)P<sub>3</sub> receptor and subtype 3 of ryanodine receptor were detected in these myocytes, and the maximal binding capacity of [<sup>3</sup>H]Ins(1,4,5)P<sub>3</sub> was 10- to 12-fold higher than that of [<sup>3</sup>H]-ryanodine. These results suggest that Ins(1,4,5)P<sub>3</sub>-gated channels mediate a continuum of Ca<sup>2+</sup> signalling in smooth-muscle cells expressing a high level of Ins(1,4,5)P<sub>3</sub> receptors and no subtypes 1 and 2 of ryanodine receptors.

**Key words:** calcium puff, calcium-release channel, confocal microscopy, sarcoplasmic reticulum, smooth muscle.

## INTRODUCTION

The release of Ca<sup>2+</sup> ions from the intracellular stores into the cytosol plays a central role in the control of many cellular activities in excitable and non-excitable cells. Ins(1,4,5)P<sub>3</sub> receptors and ryanodine receptors represent the two major types of intracellular Ca<sup>2+</sup>-release channels, and share some functional similarities. Global Ca<sup>2+</sup> signals in intact cells have been reported to be due to the co-ordinated recruitment of 'elementary' Ca<sup>2+</sup>-release units [1,2], inducing either Ca<sup>2+</sup> sparks when the units contain mainly ryanodine receptors, i.e. in cardiac and vascular myocytes [3–5], or Ca<sup>2+</sup>-release signals, or 'puffs', when the units contain mainly Ins(1,4,5)P<sub>3</sub> receptors, i.e. in *Xenopus* oocytes and HeLa cells [6,7]. Elementary Ca<sup>2+</sup> events are spatially localized, short transient signals that dissipate rapidly due to diffusion of Ca<sup>2+</sup> into the cytoplasm and sequestration into the intracellular stores.

In smooth muscles, it is believed generally that Ca<sup>2+</sup> release from the intracellular store can be generated by Ins(1,4,5)P<sub>3</sub> and ryanodine receptors [8]. In rat portal-vein myocytes, there are indications that these two Ca<sup>2+</sup>-release channels are co-localized on the same intracellular store [9]. In these myocytes, ryanodine receptors are highly expressed and organized in clustered units, so that they can generate Ca<sup>2+</sup> sparks. In contrast, Ins(1,4,5)P<sub>3</sub> receptors are not organized in clustered units and Ins(1,4,5)P<sub>3</sub>-evoked Ca<sup>2+</sup> puffs have not been observed in portal-vein myocytes [9]. Up to now, Ca<sup>2+</sup> puffs activated by Ins(1,4,5)P<sub>3</sub> have never been reported in any smooth muscle. On the basis of contraction and cytosolic Ca<sup>2+</sup> measurements, it has

been suggested recently that rat ureter myocytes may possess only an Ins(1,4,5)P<sub>3</sub>-sensitive Ca<sup>2+</sup> store [10,11] and may therefore represent a good model with which to study the hierarchy of Ca<sup>2+</sup> signals evoked by Ins(1,4,5)P<sub>3</sub>-gated channels.

The present study identifies for the first time in smooth-muscle cells Ca<sup>2+</sup> puffs evoked by activation of clusters of Ins(1,4,5)P<sub>3</sub>-gated channels in response to photorelease of Ins(1,4,5)P<sub>3</sub> and application of low doses of acetylcholine. Ca<sup>2+</sup> puffs can be observed spontaneously in Ca<sup>2+</sup>-overloaded myocytes. The Ca<sup>2+</sup> puffs display some variability in size, time course and spatial spread. Increasing concentrations of Ins(1,4,5)P<sub>3</sub> and acetylcholine induce a spatial recruitment of localized Ca<sup>2+</sup> signals leading to propagated Ca<sup>2+</sup> waves. The functional experiments are supported by immunodetection of Ins(1,4,5)P<sub>3</sub> receptors, showing the existence of several spots of fluorescence in confocal cell sections, and by binding data indicating that the density of Ins(1,4,5)P<sub>3</sub> receptors is 10–12-fold higher than that of ryanodine receptors in these myocytes. These results suggest that in visceral smooth-muscle cells expressing a high level of Ins(1,4,5)P<sub>3</sub> receptors and no subtypes 1 and 2 of ryanodine receptors, a continuum of Ins(1,4,5)P<sub>3</sub>-gated channel-mediating Ca<sup>2+</sup> signalling can be detected.

## EXPERIMENTAL PROCEDURES

### Cell preparation, solutions and membrane-current recordings

Wistar rats (150–160 g) were stunned and killed by cervical dislocation. Ureters were removed quickly, cut into several pieces and incubated for 10 min in low-calcium (40 μM) physiological

Abbreviations used: AM, acetoxymethyl ester; [Ca<sup>2+</sup>]<sub>i</sub>, cytoplasmic calcium concentration; [Ca<sup>2+</sup>]<sub>o</sub>, external calcium concentration; FWHM, full width at half-maximal amplitude; Fluo-3, 1-[2-amino-5-(2,7-dichloro-6-hydroxy-3-oxo-3H-xanthen-9-yl)]-2-(2'-amino-5'-methylphenoxy)ethane-*N,N,N',N'*-tetra-acetic acid penta-ammonium; Indo-1, 1-[2-amino-5-(6-carboxyindol-2-yl)phenoxy]-2-(2'-amino-5'-methylphenoxy)ethane-*N,N,N',N'*-tetra-acetic acid pentasodium.

<sup>1</sup> To whom correspondence should be addressed (e-mail jean.mironneau@umr5017.u-bordeaux2.fr).

solution; then 0.8 mg/ml collagenase, 0.25 mg/ml Pronase E and 1 mg/ml BSA were added at 37 °C for 15 min. After this time, the solution was removed and the ureter pieces were incubated again in a fresh enzyme solution at 37 °C for 15 min. Tissues were then placed in enzyme-free solution and triturated using a fire-polished Pasteur pipette to release cells. Cells were stored on glass coverslips and used within 10 h. Portal-vein myocytes were obtained as described previously [5,9].

The normal physiological solution used contained 130 mM NaCl, 5.6 mM KCl, 1 mM MgCl<sub>2</sub>, 1.7 mM CaCl<sub>2</sub>, 11 mM glucose and 10 mM Hepes, pH 7.4. The basic pipette solution contained 130 mM CsCl, 10 mM Hepes and 60 μM Fluo-3 {1-[2-amino-5-(2,7-dichloro-6-hydroxy-3-oxo-3H-xanthen-9-yl)]-2-(2'-amino-5'-methylphenoxy)ethane-*N,N,N',N'*-tetra-acetic acid penta-ammonium}, pH 7.3, with CsOH. Substances were applied externally by pressure ejection from a glass pipette for the periods indicated in the relevant Figure legends. All the experiments were performed at 28 ± 1 °C.

Voltage-clamp and membrane-current recordings were made with a standard patch-clamp technique using a List EPC-7 patch-clamp amplifier (List, Darmstadt-Eberstadt, Germany). Patch pipettes had resistances of 4–6 MΩ. Membrane potential and whole-cell membrane current were stored and analysed using an IBM-PC computer (P-clamp System, Axon Instruments, Foster City, CA, U.S.A.).

### Confocal microscopy and fluorescence measurements

A Bio-Rad MRC 1000 (Bio-Rad, Paris, France) confocal scanning head was coupled to a Nikon Diaphot (Nikon, Tokyo, Japan) inverted microscope. In all experiments a Nikon Plan Apo × 60, 1.4 numerical aperture objective lens was used. The iris aperture was set to 40–50% of maximum, providing an axial (*z*) resolution of about 1.5 μm and an *x-y* resolution of 0.4 μm. Illumination was provided by a 25-mW argon ion laser (Ion Laser Technology, Salt Lake City, UT, U.S.A.). The excitation wavelength (488 nm) was selected using interference filters and the emitted fluorescence was collected at wavelengths greater than 515 nm. For some experiments, Fluo-3 (60 μM) was dialysed into the cells through the patch-pipette, as reported previously [9]. The fluorescence beam was filtered and detected using a photomultiplier tube. For other experiments, cells were loaded by incubation in physiological solution containing 1 μM Fluo-3 acetoxymethyl ester (AM) for 1 h at room temperature. These cells were washed and allowed to cleave the dye to the active Fluo-3 compound for at least 1 h. To compensate for uneven distribution of the Fluo-3, self ratios were calculated ( $R = F/F_{\text{rest}}$ , where *F* is fluorescence and *F*<sub>rest</sub> is resting-level fluorescence). Note that no change in fluorescence corresponds to  $F/F_{\text{rest}} = 1$  and  $\Delta F/F_{\text{rest}} = 0$ . Image acquisition and data analysis were performed by using COMOS, TCSM and MPL-1000 software (Bio-Rad). Images were acquired in the line-scan mode of the confocal microscope; this mode repeatedly scanned a single line through the cell every 6 ms. Spatial average fluorescence can be measured (after filtering with a 3 × 3 rank filter) in the entire line-scan image or in a 2-μm region on the *x*-axis, illustrating temporal changes of [Ca<sup>2+</sup>]<sub>i</sub>, the cytoplasmic calcium concentration.

In some experiments, cells were loaded by incubation in physiological solution containing 1 μM Indo-1 {1-[2-amino-5-(6-carboxyindol-2-yl)phenoxy]-2-(2'-amino-5'-methylphenoxy)-ethane-*N,N,N',N'*-tetra-acetic acid pentasodium}/AM for 30 min. Measurement of fluorescence to monitor [Ca<sup>2+</sup>]<sub>i</sub> using Indo-1 has been reported previously [12].

### Flash photolysis

Caged Ins(1,4,5)P<sub>3</sub> [Ins(1,4,5)P<sub>3</sub>, P<sup>4(6)</sup>-1-(2-nitrophenyl) ethyl ester] was introduced into the cell via the patch pipette, allowing 3–4 min for equilibration. Photolysis was produced by a 1-ms pulse from a xenon flash lamp (Hi-Tech Scientific, Salisbury, Wilts., U.K.) focused to a spot of about 2 mm in diameter around the cell. Light was band-pass filtered with a UG11 glass between 300 and 350 nm. Flash intensity could be adjusted by varying the capacitor charging voltage between 0 and 385 V, which corresponded to a change in the energy input into the flash lamp from 0 to 240 J. Upon flash photolysis, Ins(1,4,5)P<sub>3</sub> was released within 2 ms. A small percentage of conversion of caged compounds (about 10%) was useful if repetitive pulses were applied in order to obtain similar responses. Flash intensities up to 60 J could be applied repetitively without altering the reserve of caged Ins(1,4,5)P<sub>3</sub> (20 μM) and, consequently, the amount of photoreleased compounds.

### Immunocytochemistry

Myocytes were immunostained as described previously [13], except that donkey serum was used instead of fetal calf serum. Myocytes were incubated in the presence of anti-Ins(1,4,5)P<sub>3</sub> receptor antibodies (at 1:200 dilution) for 20 h at 4 °C, and the secondary antibodies (donkey anti-rabbit IgG conjugated to FITC, diluted 1:200) were incubated for 3 h at 20 °C. Thereafter, cells were mounted in Vectashield.

### Microsomal-membrane preparation

Microsomal membranes of ureter and cerebellum from Wistar rats were prepared by homogenization with a Kontes potter in a solution containing 20 mM Tris/HCl, 1 mM EGTA and 1 mM PMSF, pH 7.4. The homogenate was centrifuged at 170 *g* for 10 min at 4 °C. Microsomal membranes were obtained as a pellet by centrifugation of the supernatant at 185000 *g* for 90 min at 4 °C. Microsomal membranes were then resuspended in the buffer and stored at –80 °C. Protein concentration was determined according to Bradford [14].

### Immunoblotting

For Western-blotting analysis, microsomal proteins were separated on SDS/PAGE (7.5%) minigels and transferred to PVDF membranes for 16 h at 30 V in a transfer buffer containing 192 mM glycine and 25 mM Tris/HCl (pH 8.3). Membranes were blocked for 1 h in blocking buffer containing 20 mM Tris/HCl and 3% BSA (pH 7.4) and then incubated for 5 h at room temperature with the primary anti-Ins(1,4,5)P<sub>3</sub> receptor antibody at 1:200 dilution. After extensive washing, membranes were incubated for 2 h with the secondary antibody coupled to horseradish peroxidase (anti-rabbit, 1:5000 dilution). Specific antigen detection was performed using H<sub>2</sub>O<sub>2</sub> and diaminobenzidine to detect horseradish peroxidase activity on PVDF membranes and Kodak EDAS 120 (Kodak, Rochester, NY, U.S.A.).

### [<sup>3</sup>H]Ryanodine- and [<sup>3</sup>H]Ins(1,4,5)P<sub>3</sub>-binding assays

[<sup>3</sup>H]Ryanodine binding to microsomal membranes of rat ureters was measured, as reported previously on rat portal vein [15], in a medium containing 1 M KCl, 25 mM Hepes (pH 7.8 at 37 °C), 1 mM dithiothreitol, 0.1 mM CaCl<sub>2</sub>, 1 mg/ml BSA and 0.1 mM PMSF. [<sup>3</sup>H]Ryanodine was used in the concentration range of

2–30 nM. After a 3-h incubation at 37 °C, aliquots were filtered through Whatmann GF/C fibre-glass filters and washed three times with 5 ml of ice-cold binding buffer. The filters were placed in scintillation vials filled with 4 ml of liquid-scintillation cocktail, shaken for 1 h, and counted in a Packard 1500 Tri-Carb. Non-specific binding was measured in the presence of 10  $\mu$ M ryanodine and was subtracted before calculation. At 20 nM [ $^3$ H]ryanodine, non-specific binding was < 60% of total binding.

[ $^3$ H]Ins(1,4,5) $P_3$  binding was measured in a medium containing 0.1 M KCl, 50 mM Tris/HCl (pH 8.3 at 2–4 °C) and 1 mM EGTA. [ $^3$ H]Ins(1,4,5) $P_3$  was used in the concentration range of 2–200 nM. After a 10-min incubation on ice, binding reactions were terminated by centrifugation (15000 g, 15 min, 4 °C). The supernatant was aspirated and the pellet was rinsed quickly with 0.2 ml of ice-cold binding buffer. Pellets were solubilized with 0.1 ml of Soluene-100 (55 °C, 30 min). After transfer into scintillation vials with 4 ml of liquid-scintillation cocktail, radioactivity was counted in a Packard 1500 Tri-Carb. Non-specific binding was measured in the presence of a 1000-fold excess of Ins(1,4,5) $P_3$  over [ $^3$ H]Ins(1,4,5) $P_3$  concentration. At 100 nM [ $^3$ H]Ins(1,4,5) $P_3$ , non-specific binding was < 55% of total binding.

Maximal binding capacity ( $B_{max}$ ) and dissociation constant ( $K_d$ ) were obtained from saturation binding experiments.

### Reverse transcriptase PCR

Total RNA was extracted from about 500 cells using the RNeasy mini kit (Qiagen, Hilden, Germany). The reverse-transcription reaction was performed using the Sensiscript RT kit (Qiagen). Total RNA was incubated first with random primers (Promega, Lyon, France) at 65 °C for 5 min, then, after a cooling time of 15 min (at 25 °C), reverse transcriptase mix was added and the total mixture was incubated 60 min at 37 °C. The resulting cDNA was stored at –20 °C. PCR was performed with 2  $\mu$ l of cDNA (in reverse transcriptase PCR mix), 1.25 units of HotStart *Taq* DNA polymerase (Qiagen), 1  $\mu$ M of each primer and 200  $\mu$ M of each deoxynucleotide triphosphate, in a final volume of 50  $\mu$ l. The solution was supplemented with 2.5 mM MgCl<sub>2</sub>, except for subtype 1 of Ins(1,4,5) $P_3$  receptors. The PCR conditions were 95 °C for 15 min, then 35 cycles at 94 °C for 1 min, 60 °C (subtypes 1 and 2 of ryanodine receptors and all subtypes of Ins(1,4,5) $P_3$  receptors) or 56 °C (subtype 3 of ryanodine receptor) for 1 min and 72 °C for 1.5 min and at the end of PCR, samples were kept at 72 °C for 10 min for final extension and then stored at 4 °C. Reverse transcription and PCR were performed with a thermal cycler (Techne, Cambridge, U.K.). Amplification products were separated by electrophoresis (2% agarose gel) and visualized by ethidium bromide staining. Gels were photographed with EDAS 120 and analysed with KDS 1D 2.0 software (Kodak Digital Science, Paris, France). Sense and antisense primer pairs used to amplify fragments of subtypes 1, 2 and 3 of Ins(1,4,5) $P_3$  and ryanodine receptors were designed on the basis of the known cloned receptor sequences deposited in GenBank (accession numbers J05510, X61677, L06096, X83932, X83933 and X83934, respectively) with DNASTAR software (Lasergene, DNASTAR, Madison, WI, U.S.A.). The nucleotide sequences and the lengths of the expected PCR products (in parentheses) for each primer pair were as follows. Subtype 1 of Ins(1,4,5) $P_3$  receptor, sense, 5'-ACTGGAAGACCATAAAAGGGGTGA-3', and antisense, 5'-TCCGTCAGCCGCGCAGAAAATGAG-3' (368 bp); subtype 2 of Ins(1,4,5) $P_3$  receptor, sense, 5'-GGCACAGCCTCTCC-ATGTGGCAGG-3', and antisense, 5'-TTCCTGTCTCGCTG-ACCCAGTGC-3' (197 bp); subtype 3 of Ins(1,4,5) $P_3$  receptor, sense, 5'-CACGGAGCTGCCACATTTATGGGC-3', and anti-

sense, 5'-TCCTCAGTCCGTGGTTCATGACGG-3' (168 bp) [16]; subtype 1 of ryanodine receptor, sense, 5'-GAAGGTTCTGGACAAACACGGG-3', and antisense, 5'-TCGCTCTTGT-TGTAGAATTTGCGG-3' (435 bp); subtype 2 of ryanodine receptor, sense, 5'-GAATCAGTGAGTTACTGGGCATGG-3', and antisense, 5'-CTGGTCTCTGAGTTCTCCAAAAGC-3' (635 bp); subtype 3 of ryanodine receptor, sense, 5'-CCTTCG-CTATCAACTTCATCCTGC-3', and antisense, 5'-TCTTCTA-CTGGGCTAAAGTCAAGG-3' (505 bp) [17].

### Chemicals and drugs

Collagenase was obtained from Worthington (Freehold, NJ, U.S.A.); Pronase E, BSA, acetylcholine, heparin and Ins(1,4,5) $P_3$  were from Sigma (St Louis, MO, U.S.A.). Ryanodine, Indo-1/AM and caged Ins(1,4,5) $P_3$  [Ins(1,4,5) $P_3$ ,  $P^{1(6)}$ -1-(2-nitrophenyl)ethyl ester] were from Calbiochem (Meudon, France). Caffeine was from Merck (Nogent sur Marne, France). Fluo-3 and Fluo-3/AM were from Molecular Probes Europe (Leiden, The Netherlands). Oxodipine was a gift from Dr Galiano (Instituto de Investigacion y Desarrollo Quimico Biologico, Madrid, Spain). [ $^3$ H]Ryanodine (68 Ci/mmol) and [ $^3$ H]Ins(1,4,5) $P_3$  (20 Ci/mmol) were from DuPont NEN (Boston, MA, U.S.A.). Primers specific for Ins(1,4,5) $P_3$  and ryanodine receptors were synthesized by Eurogentec (Seraing, Belgium).

Antibodies directed against Ins(1,4,5) $P_3$  and ryanodine receptors were added to the pipette solution to allow dialysis of the cell after a breakthrough in whole-cell recording mode for at least 5–8 min, a time longer than that expected theoretically for diffusion of substances in solutions [18]. The rabbit anti-Ins(1,4,5) $P_3$ -receptor antibody was raised to the C-terminal amino acids (GGVGDVLRKPS) of the Ins(1,4,5) $P_3$  receptors (407143-S, Calbiochem). The mouse anti-(ryanodine receptor) antibody was raised to the C-terminal amino acids (DQQEQV-KEDMETK) of the ryanodine receptor (559279-S, Calbiochem). For immunological detection, FITC-conjugated affinity-pure donkey anti-rabbit IgG and donkey serum were from Jackson ImmunoResearch Laboratories (West Grove, PA, U.S.A.) and Vectashield was from Biosys (Compiègne, France).

### Analysis of data

The results are expressed as means  $\pm$  S.E.M. Significance was tested by means of Student's *t* test. *P* values of < 0.05 were considered significant.

## RESULTS

### Expression of Ins(1,4,5) $P_3$ and ryanodine receptors in rat ureteric myocytes

The expression of Ins(1,4,5) $P_3$ - and ryanodine-receptor subtypes was examined by using subtype-specific primers designed to amplify cDNA fragments of subtypes 1, 2 and 3 of these receptors in rat ureter and cerebellum. Amplified fragments of all three Ins(1,4,5) $P_3$ -receptor subtypes were observed (Figure 1A), indicating that the three Ins(1,4,5) $P_3$ -receptor mRNAs were expressed in ureter and cerebellum. In contrast, amplification of fragments of mRNAs encoding the ryanodine-receptor subtypes showed that only the subtype 3 was expressed in rat ureteric myocytes, whereas all three subtypes were revealed in cerebellum (Figure 1B). Amplified products obtained with the primers designed to amplify the Ins(1,4,5) $P_3$ - or ryanodine-receptor subtypes displayed sizes and sequences (results not shown) corresponding to those of the cloned Ins(1,4,5) $P_3$ - or ryanodine-receptor subtypes. Scatchard analysis of [ $^3$ H]Ins(1,4,5) $P_3$  and

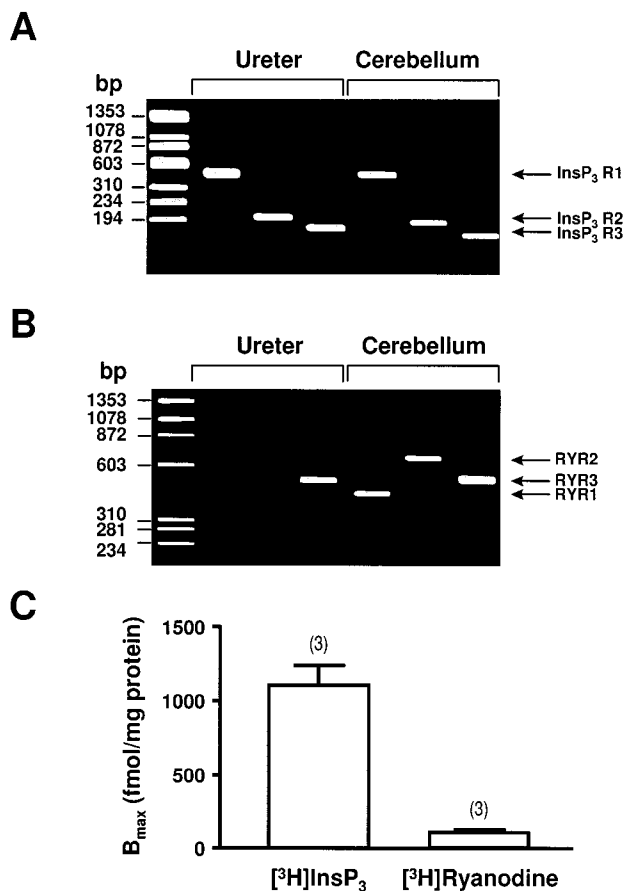


**Figure 1** Expression of Ins(1,4,5) $P_3$  and ryanodine receptors in rat ureteric myocytes

(A) Amplified DNA fragments of subtypes 1, 2 and 3 (R1–3) of Ins(1,4,5) $P_3$  receptors were separated on a 2% agarose gel and visualized by staining with ethidium bromide using rat ureter and cerebellum RNA. Numbers on the left indicate molecular-size standards. (B) Amplified DNA fragments of isoforms 1, 2 and 3 of ryanodine receptors (RYR1–3) using rat ureter and cerebellum RNA. For RNA purification and PCR conditions, see the Experimental procedures section. (C) Specific binding of [ $^3$ H]Ins(1,4,5) $P_3$  and [ $^3$ H]ryanodine to ureteric smooth-muscle membranes. Maximal binding capacity ( $B_{max}$ ) corresponding to the total number of binding sites (high-affinity sites for [ $^3$ H]ryanodine; high-affinity plus low-affinity sites for [ $^3$ H]Ins(1,4,5) $P_3$ ) is the mean  $\pm$  S.E.M. of three experiments, each carried out in duplicate. The mean  $K_D$  values for [ $^3$ H]ryanodine and [ $^3$ H]Ins(1,4,5) $P_3$  (high-affinity and low-affinity) were 2.5, 5.3 and 207.5 nM, respectively.

[ $^3$ H]ryanodine binding on rat ureter membranes showed that the  $B_{max}$  value corresponding to the total number of Ins(1,4,5) $P_3$ -binding sites (high-affinity plus low-affinity sites) was  $1113 \pm 125$  fmol/mg of protein ( $n = 3$ ), whereas the  $B_{max}$  value corresponding to the total number of ryanodine-binding sites was  $109 \pm 21$  fmol/mg of protein ( $n = 3$ ; Figure 1C). Finally, Western-blot detection on samples of rat ureter and cerebellum (Figure 2A) revealed a similar molecular-mass band ( $\approx 240$  kDa) corresponding to the value reported previously for Ins(1,4,5) $P_3$  receptors [19]. These results indicate that rat ureteric myocytes possess mainly Ins(1,4,5) $P_3$  receptors.

Immunodetection of Ins(1,4,5) $P_3$  receptors in 0.5- $\mu$ m confocal sections from freshly dissociated ureteric myocytes was performed with the anti-[Ins(1,4,5) $P_3$  receptor] antibody (used for protein detection) and the binding sites were revealed with FITC-conjugated secondary antibody. As illustrated in Figure 2(B), Ins(1,4,5) $P_3$  receptors appeared to be distributed in the whole

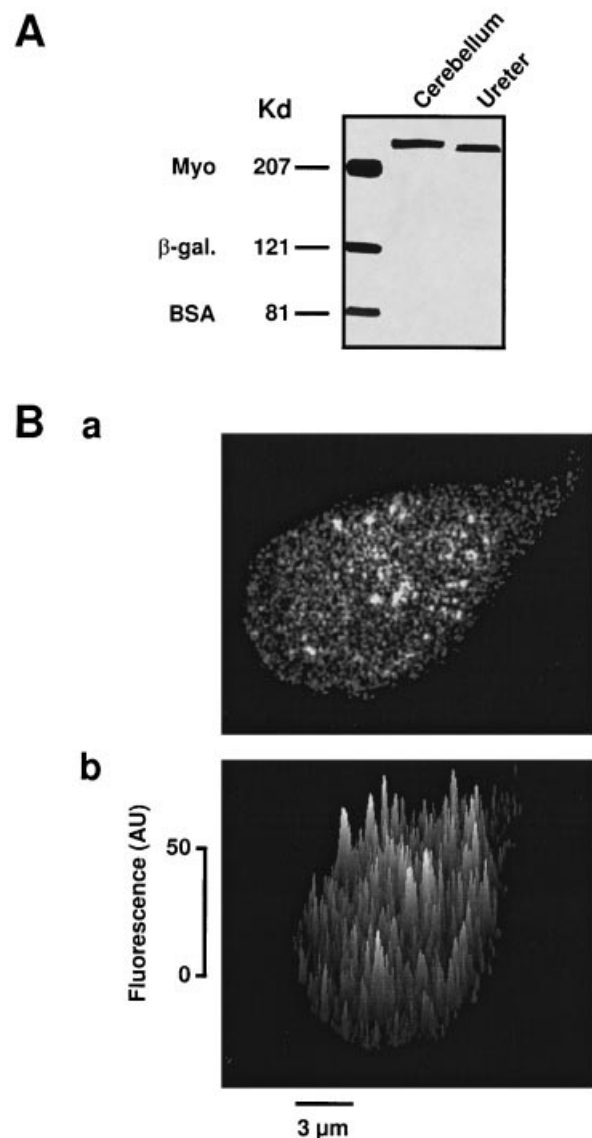


**Figure 2** Immunological detection of Ins(1,4,5) $P_3$  receptors in rat ureteric myocytes

(A) Microsomes of ureter smooth muscle (200  $\mu$ g) and cerebellum (100  $\mu$ g) were separated by SDS/PAGE (7.5% gel) and analysed by Western blot with an anti-Ins(1,4,5) $P_3$ -receptor antibody. Numbers on the left indicate molecular-mass standards (in kDa). Myo, myosin;  $\beta$ -gal,  $\beta$ -galactosidase. (B) Immunolocalization of Ins(1,4,5) $P_3$  receptors. (a) A typical confocal cell section of a freshly dissociated ureteric myocyte performed above the nucleus, showing several spots of fluorescence near the plasma membrane and in the cytoplasm. (b) Three-dimensional representation of the fluorescence (in arbitrary units, AU) from the same confocal cell section. In absence of primary antibody or after inactivation of the antibody with its antigen, only a faint background fluorescence was observed.

confocal section, with several marked spots of fluorescence localized near the plasma membrane and in the cytoplasm. Taken together, these results suggest that ureter smooth muscle can be a suitable model for studying  $Ca^{2+}$  signalling induced by Ins(1,4,5) $P_3$ -gated channels.

#### Acetylcholine- and Ins(1,4,5) $P_3$ -induced localized $Ca^{2+}$ signals

Line-scan images of ureteric myocytes were obtained by scanning of a single line in a confocal section. Most of the scanned lines

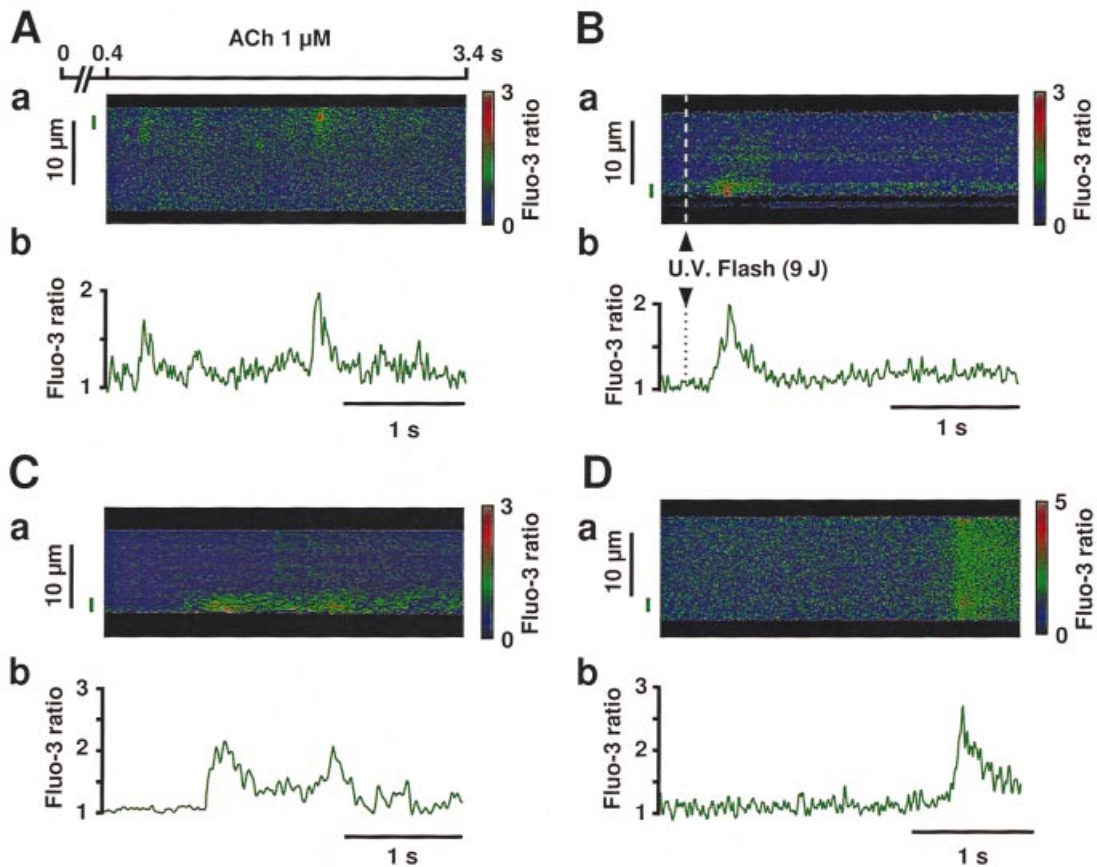


**Figure 3** Triggered and spontaneous  $Ca^{2+}$ -release signals in rat ureteric myocytes

(A) Typical  $Ca^{2+}$  response evoked by  $1 \mu M$  acetylcholine (ACh; horizontal bar) in physiological ( $1.7 \text{ mM } Ca^{2+}$ ) solution, shown as a line-scan image (a) and averaged fluorescence from a  $2\text{-}\mu m$  region (b), indicated by the vertical bar on the line-scan image. Myocytes were loaded with Fluo-3/AM and not patch-clamped. (B)  $Ca^{2+}$  responses evoked by a 9-J flash pulse in physiological solution, displayed as in (A), indicated by the vertical bar on the line-scan image. Myocytes were loaded with Fluo-3 and caged Ins(1,4,5) $P_3$  through the patch-pipette and held at  $-50 \text{ mV}$ . (C, D) Spontaneous  $Ca^{2+}$  puff (C) and  $Ca^{2+}$  spike (D), displayed as in (A), indicated by the vertical bar on the line-scan image in myocytes superfused with  $10 \text{ mM } Ca^{2+}$  from 30 min. Myocytes were loaded with Fluo-3/AM and not patch-clamped. External solution contained  $10 \mu M$  ryanodine and  $1 \mu M$  oxodipine. No change in fluorescence corresponds to a Fluo-3 ratio of 1.

performed above the nucleus detected  $Ca^{2+}$  signals, in agreement with immunostaining of Ins(1,4,5) $P_3$  receptors (Figure 2B). Experiments were performed in either voltage-clamped (holding potential,  $-50 \text{ mV}$ ) or non-voltage-clamped myocytes, in the continuous presence of  $1 \mu M$  oxodipine (a light-stable dihydropyridine) to inhibit voltage-dependent  $Ca^{2+}$  channels. Fluorescence signals are expressed as a pseudo-ratio ( $F/F_{rest}$ ) and are depicted by a pseudocolour scale as indicated by the colour bars (see Figures 3 and 5, below). The basal  $[Ca^{2+}]_i$  level measured with the Indo-1 dye was  $91 \pm 7 \text{ nM}$  ( $n = 25$ ).

In non-voltage-clamped ureteric myocytes, applications of  $1 \mu M$  acetylcholine induced localized and transient  $Ca^{2+}$  signals that originated from 1 or 2 initiation sites in the line-scan images and appeared after a delay of  $0.55 \pm 0.01 \text{ s}$  ( $n = 29$ ; Figure 3A). However, these signals showed some heterogeneity in amplitude, time course and spatial spread, even when they originated from the same site. The largest  $Ca^{2+}$ -release events are characterized by a relatively rapid upstroke (with time-to-peak of  $93.6 \pm 9.7 \text{ ms}$ ,  $n = 10$ ) followed by a decline, with a time to decay to half-maximal amplitude of  $107.4 \pm 16.4 \text{ ms}$ , and were restricted to a small area with full width at half-maximal amplitude (FWHM) of  $1.89 \pm 0.23 \mu m$ . The peak amplitude of such events was  $1.13 \pm 0.16$  ( $\Delta F/F_{rest}$ ,  $n = 10$ ) and they appear generally similar to the  $Ca^{2+}$  puffs reported in non-excitable cells [6,7]. The smallest

$Ca^{2+}$ -release events had a lower peak amplitude ( $\Delta F/F_{rest} = 0.39 \pm 0.02$ ,  $n = 19$ ) and a more restricted spatial spread ( $1.03 \pm 0.07 \mu m$ ). The kinetics of these events were more rapid than those of  $Ca^{2+}$  puffs, with time-to-peak and time at half-decay of  $49.2 \pm 3.9 \text{ ms}$  and  $60.9 \pm 8.5 \text{ ms}$ , respectively ( $n = 19$ ). Such small events are unlikely to be due to out-of-focus  $Ca^{2+}$  puffs, since such out-of-focus  $Ca^{2+}$  signals would exhibit a reduced amplitude and a slower time course [20], whereas the detected small events are generally much faster than the other localized  $Ca^{2+}$  events.

Distributions of peak fluorescence, time-to-peak, time at half-decay and FWHM of 29 elementary  $Ca^{2+}$  signals obtained from 11 different cells are illustrated in Figure 4. The broad range of amplitude, time-to-peak, time at half-decay and FWHM is consistent with the notion of a continuum of  $Ca^{2+}$  puffs rather than a hierarchy of discrete amplitudes. This conclusion is also supported by the localization of  $Ca^{2+}$  events of different amplitude originating from the same site (Figure 3A). In addition, a noticeable variation was also observed in spatial spread (Figure 4D). Such a variation in FWHM would be expected for  $Ca^{2+}$  events that differed in amplitude, since a high-amplitude signal should have a larger spatial spread than a signal of lower amplitude, providing the  $Ca^{2+}$  buffering and sequestration mechanisms were equal for both events. As shown in Figure 4(D)

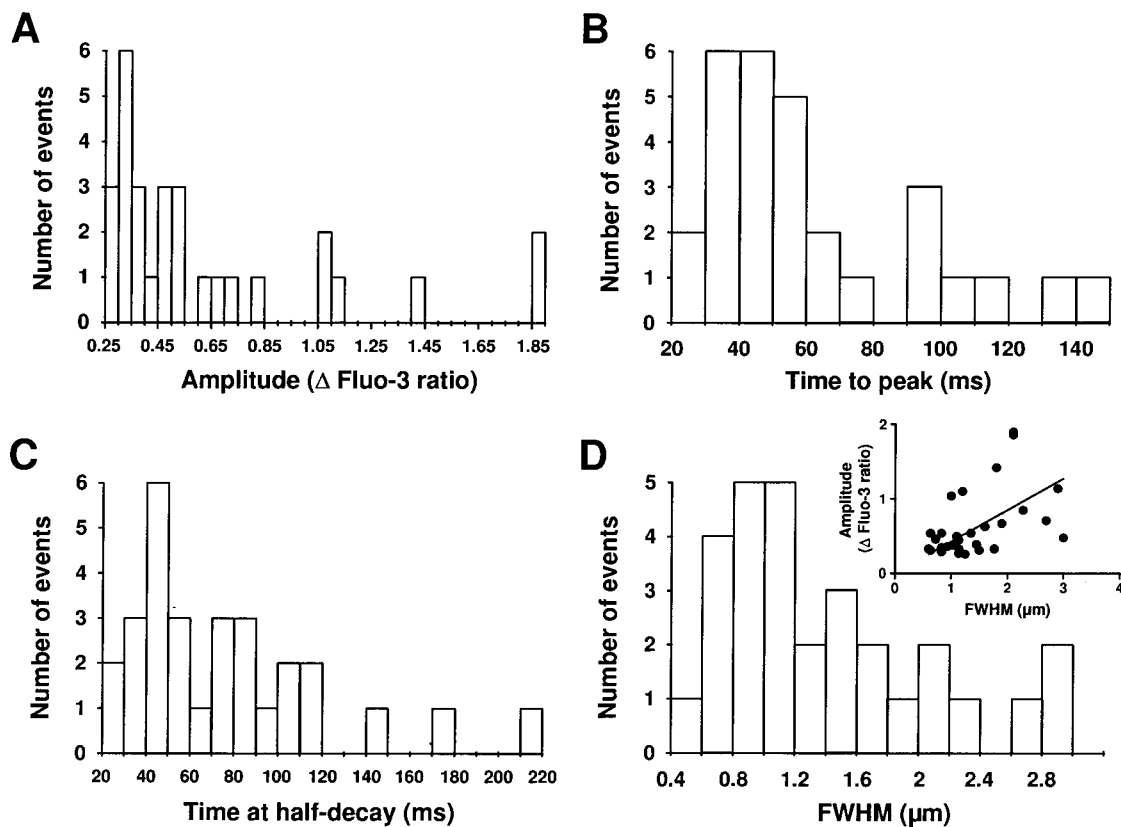


**Figure 4** Characteristics of localized  $\text{Ca}^{2+}$ -release signals evoked by low concentrations of acetylcholine

(A) Amplitude histogram of 29 elementary  $\text{Ca}^{2+}$  signals (from 11 different cells) stimulated by  $1 \mu\text{M}$  acetylcholine. Distribution of the time to reach peak  $\text{Ca}^{2+}$  signals (B), the time to reach half-decay (C) and the FWHM (D) for the same 29 elementary  $\text{Ca}^{2+}$  signals. Inset shows the correlation between amplitude of localized  $\text{Ca}^{2+}$  signals and FWHM. The linear regression coefficient ( $r^2$ ) was 0.72. Myocytes were loaded with Fluo-3/AM and not patch-clamped. External solution contained  $1 \mu\text{M}$  oxodipine.

(inset), such a relationship between amplitude and spatial spread could be observed, although the correlation was not high ( $r^2 = 0.72$ ).

In voltage-clamped myocytes, photorelease from a caged  $\text{Ins}(1,4,5)\text{P}_3$  precursor by UV-light flashes of low-intensity (9 J) evoked localized and transient  $\text{Ca}^{2+}$  events (Figure 3B) with variable amplitudes and time courses ( $n = 15$ ), similar to those obtained with  $1 \mu\text{M}$  acetylcholine.

#### Spontaneous $\text{Ca}^{2+}$ puffs in $\text{Ca}^{2+}$ -overloaded myocytes

In accordance with previous data [21], the potency of muscle cells to generate spontaneous localized  $\text{Ca}^{2+}$  signals may depend on the  $\text{Ca}^{2+}$ -loading status. Superfusion of ureteric myocytes with  $10 \text{ mM}$   $[\text{Ca}^{2+}]_o$  (the external calcium concentration) for at least 30 min resulted in a significant increase in the mean amplitude ( $\Delta F/F_{\text{rest}}$ ) of the  $\text{Ca}^{2+}$  responses evoked by  $10 \mu\text{M}$  acetylcholine from  $2.48 \pm 0.15$  ( $n = 32$ ) in normal ( $1.7 \text{ mM}$   $\text{Ca}^{2+}$ ) physiological solution to  $2.89 \pm 0.17$  ( $n = 32$ ) in  $10 \text{ mM}$   $[\text{Ca}^{2+}]_o$ , suggesting a  $\text{Ca}^{2+}$  loading of the store. With a  $[\text{Ca}^{2+}]_o$  of  $1.7 \text{ mM}$ , most ureteric myocytes had a steady-state  $[\text{Ca}^{2+}]_i$  level and spontaneous  $\text{Ca}^{2+}$  signals were very scarce. With a  $[\text{Ca}^{2+}]_o$  of  $10 \text{ mM}$  for at least 30 min, the basal  $[\text{Ca}^{2+}]_i$  level was not significantly affected ( $97 \pm 12 \text{ nM}$ ,  $n = 20$ ) but discrete, spontaneous events occurred more frequently (Figure 3C). The majority of these localized  $\text{Ca}^{2+}$  events were not associated with  $\text{Ca}^{2+}$  waves. Occasionally, localized  $\text{Ca}^{2+}$  events appeared to spread and generate transient

$\text{Ca}^{2+}$  spikes (Figure 3D). The peak amplitude of spontaneous  $\text{Ca}^{2+}$  events was  $1.24 \pm 0.20$  ( $\Delta F/F_{\text{rest}}$ ,  $n = 31$ ). The time-to-peak, the half-time of decay and the FWHM were  $110 \pm 25$ ,  $190 \pm 35$  and  $2.51 \pm 0.25 \mu\text{m}$ , respectively ( $n = 31$ ). Although  $\text{Ca}^{2+}$  overload appeared to slow the time course of the  $\text{Ca}^{2+}$ -signal decline and to increase slightly the FWHM, the kinetic parameters of the spontaneous  $\text{Ca}^{2+}$  events resembled those of  $\text{Ca}^{2+}$  puffs. The frequency of spontaneous  $\text{Ca}^{2+}$  puffs increased significantly from  $0.03 \pm 0.01 \text{ puff} \cdot \text{s}^{-1}$  ( $n = 54$ ) in control conditions to  $0.31 \pm 0.3 \text{ puff} \cdot \text{s}^{-1}$  ( $n = 31$ ) in  $\text{Ca}^{2+}$ -loading conditions. These results show that in muscle cells overloaded with  $\text{Ca}^{2+}$ , clustered  $\text{Ins}(1,4,5)\text{P}_3$  receptors may underlie spontaneous  $\text{Ca}^{2+}$  releases, as in non-excitable cells [22]. Spontaneous  $\text{Ca}^{2+}$  puffs were obtained in the continuous presence of  $10 \mu\text{M}$  ryanodine and  $1 \mu\text{M}$  oxodipine to inhibit ryanodine receptors and L-type  $\text{Ca}^{2+}$  channels, respectively. In addition, in patch-clamped myocytes intracellular applications of  $1 \text{ mg/ml}$  heparin or  $10 \mu\text{g/ml}$  anti- $[\text{Ins}(1,4,5)\text{P}_3 \text{ receptor}]$  antibody for 7–8 min suppressed any spontaneous  $\text{Ca}^{2+}$ -release signals ( $n = 12$ ).

#### Acetylcholine- and $\text{Ins}(1,4,5)\text{P}_3$ -induced $\text{Ca}^{2+}$ waves

It is proposed generally that the spatio-temporal summation of localized  $\text{Ca}^{2+}$  signals due to  $\text{Ins}(1,4,5)\text{P}_3$ -receptor activation gives rise to the whole-cell increase in  $[\text{Ca}^{2+}]_i$ . Increases in the frequency or amplitude of localized  $\text{Ca}^{2+}$  signals, or spatial recruitment of additional initiation sites, have been reported to

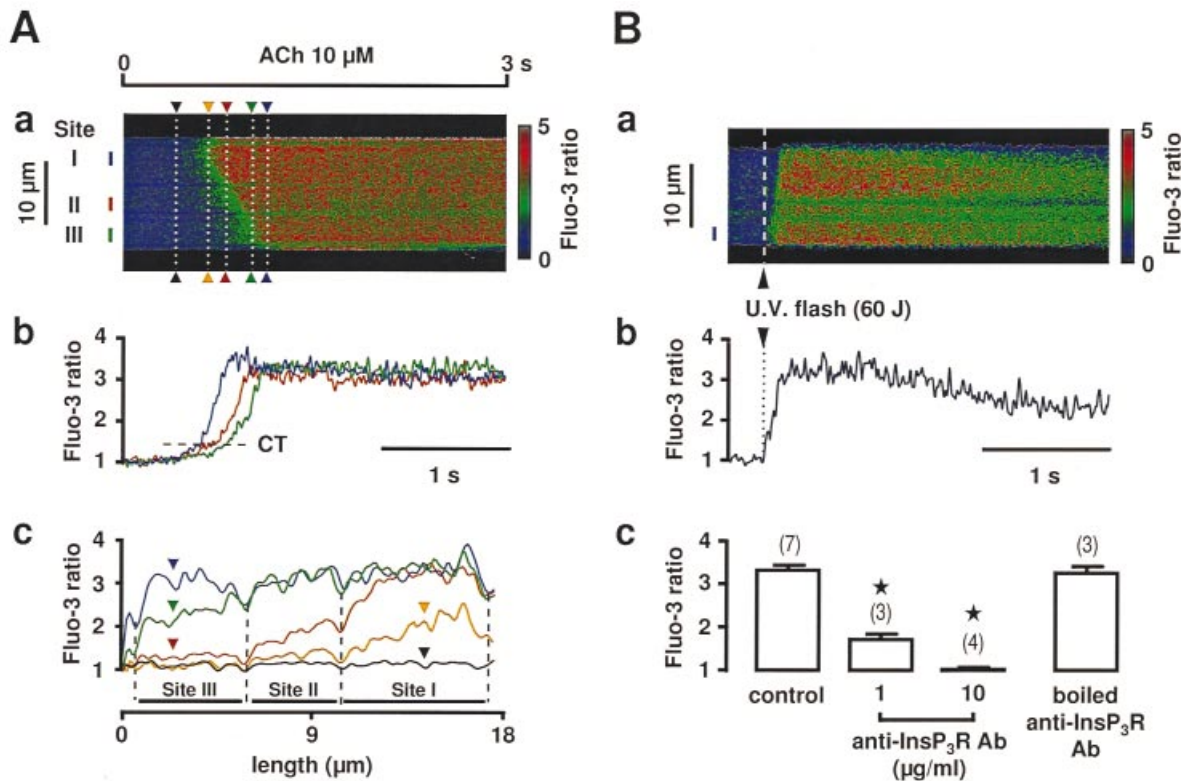


**Figure 5** Activation of propagated  $Ca^{2+}$  waves by high doses of acetylcholine (ACh) and high-intensity flash photolysis of caged Ins(1,4,5) $P_3$

(A) Line-scan image (a) in response to the continuous application of 10  $\mu$ M acetylcholine, as indicated by the horizontal bar. (b) Averaged fluorescence from three 2- $\mu$ m regions (indicated by the vertical bars on the line-scan image). CT, control [ $Ca^{2+}$ ]<sub>i</sub> threshold. (c) Spatial profiles (measured in 2- $\mu$ m-wide areas indicated by coloured arrow heads) of the line-scan image shown in (A, a). In this myocyte, the  $Ca^{2+}$  wave started at one site (site I, yellow trace) and then propagated through the entire line-scan image by recruiting neighbouring  $Ca^{2+}$ -release sites (sites II and III). Myocytes were loaded with Fluo-3/AM and not patch-clamped. (B)  $Ca^{2+}$  waves evoked by flash photolysis of caged Ins(1,4,5) $P_3$  in voltage-clamped rat ureteric myocytes. (a) Line-scan image evoked by a high-intensity (60 J) flash pulse. (b) Averaged fluorescence from a 2- $\mu$ m region indicated by the vertical bar on the line-scan image. (c) Compiled data showing the effects of the anti-Ins(1,4,5) $P_3$ -receptor [anti-Ins(1,4,5) $P_3$ R] antibody (Ab), applied intracellularly for 7–8 min. Data are means  $\pm$  S.E.M. with the number of experiments indicated in parentheses.  $\star$ , Values significantly different from those obtained under control conditions ( $P < 0.05$ ). Myocytes were loaded with Fluo-3 and caged Ins(1,4,5) $P_3$  through the patch-pipette and held at  $-50$  mV. External solution contained 1  $\mu$ M oxodipine. No change in fluorescence corresponds to a Fluo-3 ratio of 1.

be necessary for triggering propagated  $Ca^{2+}$  waves [23]. In all the cells tested ( $n = 16$ ), we never observed increases in frequency or amplitude of  $Ca^{2+}$  puffs in response to 10  $\mu$ M acetylcholine, which were able to initiate propagated  $Ca^{2+}$  waves. In contrast, propagated  $Ca^{2+}$  waves appeared from a first initiation site that progressively recruited neighbouring initiation sites by  $Ca^{2+}$  diffusion (Figure 5A). The delay between application of acetylcholine and the onset of the  $Ca^{2+}$  wave was estimated to be  $0.50 \pm 0.01$  s ( $n = 16$ ). The mean amplitude ( $\Delta F/F_{rest}$ ) and the mean overall wave velocity of the acetylcholine-evoked  $Ca^{2+}$  waves were  $2.56 \pm 0.25$  and  $38 \pm 3$   $\mu$ m/s ( $n = 16$ ), respectively. The propagation velocity of  $Ca^{2+}$  waves depends on the distance between  $Ca^{2+}$ -release sites as well as their  $Ca^{2+}$  sensitivity and the amount of  $Ca^{2+}$  released. As shown in Figure 5(Ab), recordings of localized fluorescence signals at release sites activated during  $Ca^{2+}$  wave propagation showed an initial slow  $Ca^{2+}$  elevation preceding an abrupt rise. This is consistent with the triggering of regenerative  $Ca^{2+}$  release by an early rise in [ $Ca^{2+}$ ]<sub>i</sub> resulting from summation of localized  $Ca^{2+}$  signals or from  $Ca^{2+}$  ions diffusing from neighbouring active sites. Fluorescence analysis in the spatial domain at different times during the onset of the  $Ca^{2+}$  wave (Figure 5Ac) revealed clearly the recruitment of neighbouring  $Ca^{2+}$ -release sites from the early initiation site (site I in

Figure 5Ac). The mean number of initiation sites per line-scan image was  $2.4 \pm 0.4$  ( $n = 16$ ).

Photorelease of caged Ins(1,4,5) $P_3$  by high-intensity (30–60 J) flash pulses evoked large  $Ca^{2+}$  responses that started either from a simultaneous increase in [ $Ca^{2+}$ ]<sub>i</sub> in the scanned line or from an initiation site leading to activation of a propagating wave (Figure 5B). The mean amplitudes ( $\Delta F/F_{rest}$ ) of the Ins(1,4,5) $P_3$ - and acetylcholine-evoked  $Ca^{2+}$  waves in voltage-clamped myocytes were  $2.32 \pm 0.11$  and  $2.48 \pm 0.31$  ( $n = 7$ ), respectively.

To identify the molecular nature of the  $Ca^{2+}$ -release channels involved in both Ins(1,4,5) $P_3$ - and acetylcholine-induced  $Ca^{2+}$  signals, we tested the effects of Ins(1,4,5) $P_3$ - and ryanodine-receptor inhibitors. Intracellular infusion of 1 mg/ml heparin for 7–8 min through the patch-pipette suppressed both Ins(1,4,5) $P_3$ - and acetylcholine-induced  $Ca^{2+}$  waves ( $n = 5$ ; results not shown). Similarly, intracellular application of the anti-Ins(1,4,5) $P_3$ -receptor antibody for 7–8 min inhibited in a concentration-dependent manner the  $Ca^{2+}$  responses evoked by flash photolysis of caged Ins(1,4,5) $P_3$  (Figure 5Bc) or application of 10  $\mu$ M acetylcholine (Figure 6A). This antibody-induced inhibition was specific, in as much as boiled (95  $^{\circ}$ C for 30 min) anti-Ins(1,4,5) $P_3$ -receptor antibody had no significant effect on both Ins(1,4,5) $P_3$ - and acetylcholine-activated  $Ca^{2+}$  responses (Figures

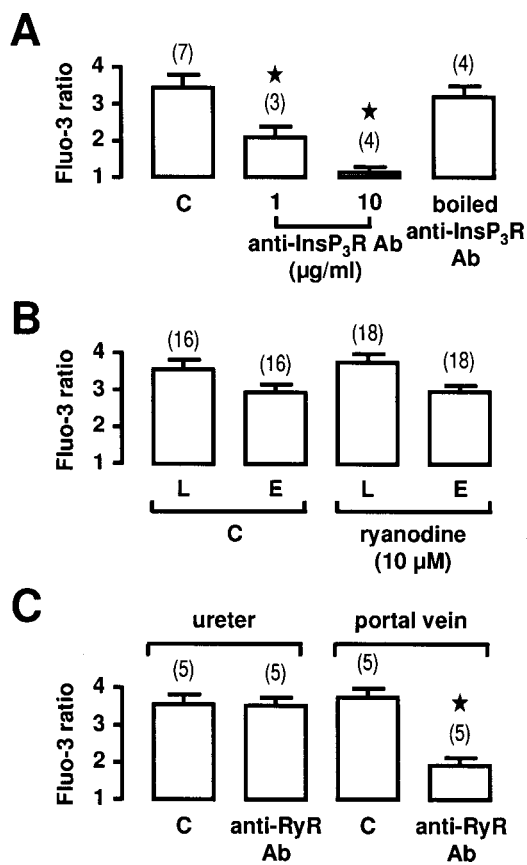


**Figure 6** Effects of inhibitors of  $\text{Ins}(1,4,5)\text{P}_3$  and ryanodine receptors on the acetylcholine-induced  $\text{Ca}^{2+}$  waves in voltage-clamped myocytes

(A) Compiled data showing the effects of increasing concentrations of anti- $\text{Ins}(1,4,5)\text{P}_3$  receptor [anti- $\text{Ins}(1,4,5)\text{P}_3\text{R}$ ] antibody (Ab) and of  $10\ \mu\text{g}/\text{ml}$  boiled antibody, applied intracellularly for 7–8 min on  $10\ \mu\text{M}$  acetylcholine-induced  $\text{Ca}^{2+}$  waves in ureteric myocytes. (B) Compiled data showing the effect of  $10\ \mu\text{M}$  ryanodine (applied externally for 15–17 min) on  $10\ \mu\text{M}$  acetylcholine-induced  $\text{Ca}^{2+}$  waves in ureteric myocytes. The fluorescence was measured either in the entire line-scan image (E) or in a localized  $2\text{-}\mu\text{m}$  region of the line-scan image (L). (C) Compiled data showing the effect of  $10\ \mu\text{g}/\text{ml}$  anti-ryanodine receptor (anti-RyR) antibody, applied intracellularly for 7–8 min on  $10\ \mu\text{M}$  acetylcholine-induced  $\text{Ca}^{2+}$  waves in ureteric and portal-vein myocytes. Data are means  $\pm$  S.E.M. with the number of cells tested indicated in parentheses. ★, Values significantly different from those obtained under control conditions ( $P < 0.05$ ). Holding potential was  $-50\ \text{mV}$ . External solution contained  $1\ \mu\text{M}$  oxidipine. No change in fluorescence corresponds to a Fluo-3 ratio of 1. C, control.

5Bc and 6A). In vascular myocytes, extracellular applications of  $10\ \mu\text{M}$  ryanodine have been shown to inhibit ryanodine receptors without depleting the internal  $\text{Ca}^{2+}$  store in a manner similar to that induced by an anti-ryanodine-receptor antibody [24]. Application of  $10\ \mu\text{M}$  ryanodine for 15–17 min in non-voltage-clamped ureteric myocytes had no significant effect on the amplitude of acetylcholine-induced global  $\text{Ca}^{2+}$  waves, measured in a  $2\text{-}\mu\text{m}$  region or in the entire line-scan image (Figure 6B). Similarly, intracellular applications of  $10\ \mu\text{g}/\text{ml}$  anti-ryanodine-receptor antibody for 7–8 min did not affect the acetylcholine-induced  $\text{Ca}^{2+}$  wave (Figure 6C) as well as the  $\text{Ins}(1,4,5)\text{P}_3$ -induced  $\text{Ca}^{2+}$  response in ureteric myocytes. In contrast, in portal-vein myocytes, the acetylcholine-induced  $\text{Ca}^{2+}$  wave was decreased by about 60% in the presence of  $10\ \mu\text{g}/\text{ml}$  of the same anti-ryanodine-receptor antibody (Figure 6C), in good agreement with previous data obtained from noradrenaline-induced  $\text{Ca}^{2+}$  response [24]. It is noteworthy that  $10\ \mu\text{M}$  anti- $\text{Ins}(1,4,5)\text{P}_3$ -

receptor antibody suppressed the  $\text{Ca}^{2+}$  puffs evoked by low concentrations of acetylcholine or  $\text{Ins}(1,4,5)\text{P}_3$  using low-intensity flashes, in all the cells tested ( $n = 12$ ). In contrast,  $10\ \mu\text{M}$  anti-ryanodine-receptor antibody was ineffective on  $\text{Ca}^{2+}$  puffs ( $n = 9$ ).

## DISCUSSION

This study describes for the first time in smooth-muscle cells the localized and transient  $\text{Ca}^{2+}$  events ( $\text{Ca}^{2+}$  puffs) evoked by  $\text{Ins}(1,4,5)\text{P}_3$ -gated channels in response to low concentrations of  $\text{Ins}(1,4,5)\text{P}_3$  either released from caged  $\text{Ins}(1,4,5)\text{P}_3$  or produced by low doses of acetylcholine. In addition, spontaneous  $\text{Ca}^{2+}$  puffs were detected frequently in myocytes overloaded with  $\text{Ca}^{2+}$ . At high concentrations of  $\text{Ins}(1,4,5)\text{P}_3$  or acetylcholine, recruitment of several localized  $\text{Ca}^{2+}$  signals generates  $\text{Ca}^{2+}$  waves that appear to propagate between several  $\text{Ca}^{2+}$ -release sites in the scanned line. The functional results are supported by both binding and immunochemical data showing that  $\text{Ins}(1,4,5)\text{P}_3$  receptors are highly expressed when compared with ryanodine receptors and that spots of  $\text{Ins}(1,4,5)\text{P}_3$  receptors are detected in several areas of the cell confocal sections.

In rat ureteric myocytes, immunodetection of  $\text{Ins}(1,4,5)\text{P}_3$  receptors in cell confocal sections showed that spots of  $\text{Ins}(1,4,5)\text{P}_3$  receptors were detected in several areas in addition to an homogeneous distribution in the whole confocal sections. This observation is in good agreement with the fact that  $\text{Ins}(1,4,5)\text{P}_3$  receptors are highly expressed in these smooth-muscle cells, as supported by binding experiments. The maximal binding capacity of  $[^3\text{H}]\text{Ins}(1,4,5)\text{P}_3$  to ureteric microsomal preparations is 10–12 times higher than that of  $[^3\text{H}]\text{ryanodine}$ . The reverse-transcriptase PCR analysis showed that the RNAs encoding the three subtypes of the  $\text{Ins}(1,4,5)\text{P}_3$  receptor and subtype 3 of the ryanodine receptor were detected in rat ureteric myocytes. However, binding experiments revealed that the level of expression of ryanodine-receptor subtype 3 was very low in these cells. This low expression level together with the fact that ryanodine-receptor subtype 3 is less sensitive to  $\text{Ca}^{2+}$ -induced channel activation than the other ryanodine-receptor subtypes [25] may explain why ryanodine and the anti-ryanodine-receptor antibody do not affect both localized and global  $\text{Ca}^{2+}$  signals evoked by flash photolysis of caged  $\text{Ins}(1,4,5)\text{P}_3$  and acetylcholine. This is in contrast with results obtained in vascular myocytes, where both ryanodine and the anti-ryanodine-receptor antibody inhibit the  $\text{Ca}^{2+}$  responses evoked by noradrenaline [24] or acetylcholine (the present study). However, in vascular myocytes the density of ryanodine receptors is 3–4 times higher than that of  $\text{Ins}(1,4,5)\text{P}_3$  receptors [24]. Taken together, these results indicate that in rat ureteric myocytes the  $\text{Ca}^{2+}$  responses to photorelease of  $\text{Ins}(1,4,5)\text{P}_3$  and acetylcholine depend only on activation of  $\text{Ins}(1,4,5)\text{P}_3$  receptors, in agreement with previous contraction experiments and  $[\text{Ca}^{2+}]_i$  measurements in intact and permeabilized rat ureteric strips [10,11]. Accordingly, both  $\text{Ins}(1,4,5)\text{P}_3$ - and acetylcholine-evoked  $\text{Ca}^{2+}$  signals were blocked by heparin and by an anti- $\text{Ins}(1,4,5)\text{P}_3$ -receptor antibody, which recognized in Western-blot analysis a molecular-mass band of about 240 kDa in rat ureter and cerebellum, but were unaffected by high concentrations of ryanodine and by an anti-ryanodine-receptor antibody.

The spatio-temporal characteristics of  $\text{Ca}^{2+}$  puffs evoked by photorelease of  $\text{Ins}(1,4,5)\text{P}_3$  or low concentrations of acetylcholine were relatively variable, suggesting that they are not stereotypic. Therefore, the variable amplitude of  $\text{Ca}^{2+}$  puffs may depend on the number and organization of the  $\text{Ins}(1,4,5)\text{P}_3$



receptors in the local volume as well as the local state of  $Ca^{2+}$  loading in the sarcoplasmic reticulum. Our results are compatible with a model where Ins(1,4,5) $P_3$ -gated  $Ca^{2+}$  channels would exist in clusters containing variable numbers of channels and that within these clusters a variable number of channels could be recruited. A similar explanation has been proposed recently in non-excitabile cells to account for hormone-evoked elementary  $Ca^{2+}$  signals [20,26]. In addition, successive activation of a given cluster of Ins(1,4,5) $P_3$  receptors may decrease the amount of  $Ca^{2+}$  locally available in this area of the sarcoplasmic reticulum and modify the amplitude of localized  $Ca^{2+}$  signals. It has been also proposed that the gating properties of Ins(1,4,5) $P_3$ -gated channels may influence the amplitude and time course of  $Ca^{2+}$  events. An interesting possibility is that the individual clusters may be composed with different subtypes of Ins(1,4,5) $P_3$  receptors, which may have different sensitivity for  $Ca^{2+}$ -dependent modulation [27]. For example, subtype 3 of the Ins(1,4,5) $P_3$  receptor does not exhibit a  $Ca^{2+}$ -dependent inhibition, whereas subtype 1 shows a bell-shaped dependence on  $[Ca^{2+}]_i$  [27,28]. Another possibility is that the gating of Ins(1,4,5) $P_3$  receptors may depend on the luminal  $Ca^{2+}$  concentration which may, in turn, regulate their sensitivity to Ins(1,4,5) $P_3$  [22,29]. In agreement with this proposal is the observation of spontaneous  $Ca^{2+}$  puffs and spikes in ureteric myocytes overloaded with 10 mM  $Ca^{2+}$  for 30 min. Spontaneous  $Ca^{2+}$  release from Ins(1,4,5) $P_3$ -sensitive  $Ca^{2+}$  stores has been reported previously from permeabilized hepatocytes overloaded with  $Ca^{2+}$  [22]. To our knowledge, spontaneous  $Ca^{2+}$  puffs have never been described in intact cells at a basal Ins(1,4,5) $P_3$  level. The possibility that spontaneous  $Ca^{2+}$  puffs may activate various membrane conductances, as shown for  $Ca^{2+}$  sparks [4,5], is under investigation. It has been shown recently that co-expression of Ins(1,4,5) $P_3$ -receptor subtypes 1 and 2 facilitates  $Ca^{2+}$  oscillations, whereas expression of Ins(1,4,5) $P_3$ -receptor subtype 3 alone generates monophasic  $Ca^{2+}$  transients [30]. Since Ins(1,4,5) $P_3$ -receptor subtypes 1 and 2 are more sensitive to Ins(1,4,5) $P_3$  and  $Ca^{2+}$  [30], it can be postulated that they are required for spontaneous  $Ca^{2+}$  puffs. In contrast, the Ins(1,4,5) $P_3$ -receptor subtype 3 is activated by higher  $[Ca^{2+}]_i$  and may participate in the acetylcholine-induced  $Ca^{2+}$  wave. Further experiments are needed to identify the expression pattern of Ins(1,4,5) $P_3$ -receptor subtypes in ureteric myocytes and their specific roles in  $Ca^{2+}$  signalling.

As illustrated in Figure 5,  $Ca^{2+}$  waves propagate throughout ureteric myocytes by alternating between regeneration at several  $Ca^{2+}$ -release sites along the scanned line and  $Ca^{2+}$  diffusion between these release sites. In HeLa cells and *Xenopus* oocytes,  $Ca^{2+}$  wave activation has been associated with an increased frequency of elementary  $Ca^{2+}$  events at a single site, with an increased amplitude of  $Ca^{2+}$  events or with the recruitment of  $Ca^{2+}$ -release sites in the spatial domain [23,31]. In ureteric myocytes,  $Ca^{2+}$  waves were triggered by activation of an initiation site, frequently located at the edge of the cell, without any detectable increase in frequency or amplitude of preceding  $Ca^{2+}$  puffs. Diffusion of  $Ca^{2+}$  from this early initiation site activated neighbouring  $Ca^{2+}$ -release sites in the scanned lines, and this may account for wave-propagation velocity in ureteric myocytes. The notion that a sub-threshold pacemaker elevation of  $[Ca^{2+}]_i$  precedes regenerative  $Ca^{2+}$  waves is not new [32], but our results emphasize further the importance of the pacemaker  $Ca^{2+}$  phase in cells expressing mainly Ins(1,4,5) $P_3$  receptors.

Visceral and vascular smooth muscles display a large variability in the type of intracellular  $Ca^{2+}$  store and in the role of these stores in initiating increase in  $[Ca^{2+}]_i$  in response to mediators and hormones. Rat portal-vein myocytes possess a single functional intracellular  $Ca^{2+}$  store on which both ryanodine and

Ins(1,4,5) $P_3$  receptors have been identified [9]. However, in these cells, only clusters of ryanodine receptors are present whereas Ins(1,4,5) $P_3$  receptors are distributed homogeneously on the sarcoplasmic reticulum, and the  $B_{max}$  value of [ $^3H$ ]ryanodine binding is 3–4 times higher than that of [ $^3H$ ]Ins(1,4,5) $P_3$  binding [24]. A physiological consequence is that a co-operativity between Ins(1,4,5) $P_3$ - and ryanodine-sensitive  $Ca^{2+}$  channels is detected in these vascular myocytes to amplify  $Ca^{2+}$  release responsible for fast propagated  $Ca^{2+}$  waves in response to neuromediators [24]. In rat mesenteric artery myocytes, it has been proposed that  $Ca^{2+}$  stores are organized into small, spatially distinct compartments [33]. When these compartments possess only ryanodine or Ins(1,4,5) $P_3$  receptors, they function as separate  $Ca^{2+}$  stores and neuromediators may only activate the Ins(1,4,5) $P_3$ -sensitive  $Ca^{2+}$  store. In contrast, when the compartments possess both ryanodine and Ins(1,4,5) $P_3$  receptors, they function as mixed  $Ca^{2+}$  stores and a co-operativity between Ins(1,4,5) $P_3$  and ryanodine receptors may be effective. In rat ureteric smooth muscle, as a consequence of the high expression of Ins(1,4,5) $P_3$  receptors and the absence of subtypes 1 and 2 of ryanodine receptors,  $Ca^{2+}$  release from the intracellular store is only activated by Ins(1,4,5) $P_3$  receptors and the amplifying mechanism is a pure Ins(1,4,5) $P_3$ -induced  $Ca^{2+}$  release. In contrast, in guinea-pig ureter, the amplifying mechanism is described as dependent only on  $Ca^{2+}$ -induced  $Ca^{2+}$  release [11]. It can be proposed that in phasic smooth muscles showing electrical pacemaker activity, the  $Ca^{2+}$ -induced  $Ca^{2+}$ -release mechanism may play a major role in modulating contraction and cell excitability, whereas in tonic smooth muscles the Ins(1,4,5) $P_3$ -induced  $Ca^{2+}$ -release mechanism predominantly controls  $Ca^{2+}$  release and contraction. Taken together, these data illustrate the variability of intracellular  $Ca^{2+}$  stores and  $Ca^{2+}$ -amplifying mechanisms in different cell types expressing different amounts of Ins(1,4,5) $P_3$  and ryanodine receptors. The results emphasize the importance of combining molecular experiments, immunostaining and functional approaches to identify the specific characteristics of  $Ca^{2+}$  signalling in each cell type studied.

In conclusion, these findings show that in rat ureteric smooth-muscle cells localized and transient  $Ca^{2+}$  events induced by the opening of clusters of Ins(1,4,5) $P_3$ -sensitive  $Ca^{2+}$ -release channels can be triggered in response to neuromediator activation or recorded spontaneously in  $Ca^{2+}$ -overloaded myocytes. They represent a continuum of  $Ca^{2+}$  signals with variable amplitude, duration and diffusion rather than a strict hierarchy of  $Ca^{2+}$  events. Propagated  $Ca^{2+}$  waves appear to result from the spatial recruitment of several  $Ca^{2+}$ -release sites by  $Ca^{2+}$  diffusion. Both  $Ca^{2+}$  signals provide an integrated mechanism to regulate contractility in smooth-muscle cells where ryanodine receptors are not or are poorly expressed.

This work was supported by grants from the Centre National de la Recherche Scientifique, the Centre National des Etudes Spatiales, and Région Aquitaine (Pôle Médicament-Santé), France. We thank V. Carricaburu for initiating us into Western blot experiments and N. Biendon for secretarial assistance.

## REFERENCES

- Lipp, P. and Niggli, E. (1996) A hierarchical concept of cellular and subcellular  $Ca^{2+}$ -signalling. *Prog. Biophys. Mol. Biol.* **65**, 265–296
- Berridge, M. J. (1997) Elementary and global aspects of calcium signalling. *J. Physiol. (London)* **499**, 291–306
- Cheng, H., Lederer, W. J. and Cannell, M. B. (1993) Calcium sparks: elementary events underlying excitation-contraction coupling in heart muscle. *Science* **262**, 740–744
- Nelson, M. T., Cheng, H., Rubart, M., Santana, L. F., Bonev, A. D., Knot, H. J. and Lederer, W. J. (1995) Relaxation of arterial smooth muscle by calcium sparks. *Science* **270**, 633–637

- 5 Mironneau, J., Arnaudeau, S., Macrez-Leprêtre, N. and Boittin, F. X. (1996)  $\text{Ca}^{2+}$  sparks and calcium waves activate different  $\text{Ca}^{2+}$ -dependent ion channels in single myocytes from rat portal vein. *Cell Calcium* **20**, 153–160
- 6 Parker, I. and Yao, Y. (1996)  $\text{Ca}^{2+}$  transients associated with openings of inositol trisphosphate-gated channels in *Xenopus* oocytes. *J. Physiol. (London)* **491**, 663–668
- 7 Bootman, M., Niggli, E., Berridge, M., and Lipp, P. (1997) Imaging the hierarchical  $\text{Ca}^{2+}$  signalling system in HeLa cells. *J. Physiol. (London)* **499**, 307–314
- 8 Somlyo, A. P. and Somlyo, A. V. (1994) Signal transduction and regulation in smooth muscle. *Nature (London)* **372**, 231–236
- 9 Boittin, F. X., Coussin, F., Macrez, N., Mironneau, C. and Mironneau, J. (1998) Inositol 1,4,5-trisphosphate- and ryanodine-sensitive  $\text{Ca}^{2+}$  release channel-dependent  $\text{Ca}^{2+}$  signalling in rat portal vein myocytes. *Cell Calcium* **23**, 303–311
- 10 Burdyla, T. V., Taggart, M. J. and Wray, S. (1995) Major difference between rat and guinea-pig ureter in the ability of agonists and caffeine to release  $\text{Ca}^{2+}$  and influence force. *J. Physiol. (London)* **489**, 327–335
- 11 Burdyla, T. V., Taggart, M. J., Crichton, C., Smith, G. L. and Wray, S. (1998) The mechanism of  $\text{Ca}^{2+}$  release from the SR of permeabilised guinea-pig and rat ureteric smooth muscle. *Biochim. Biophys. Acta* **1402**, 109–114.
- 12 Morel, J. L., Macrez-Leprêtre, N. and Mironneau, J. (1996) Angiotensin II-activated  $\text{Ca}^{2+}$  entry-induced release of  $\text{Ca}^{2+}$  from intracellular stores in rat portal vein myocytes. *Br. J. Pharmacol.* **118**, 73–78
- 13 Macrez-Leprêtre, N., Kalkbrenner, F., Schultz, G. and Mironneau, J. (1997) Distinct functions of  $G_q$  and  $G_{11}$  proteins in coupling  $\alpha_1$ -adrenoceptors to  $\text{Ca}^{2+}$  release and  $\text{Ca}^{2+}$  entry in rat portal vein myocytes. *J. Biol. Chem.* **272**, 5261–5268
- 14 Bradford, M. M. (1976) A rapid and sensitive method for the quantitation of microgram quantities of protein utilizing the principle of protein-dye binding. *Anal. Biochem.* **72**, 248–254
- 15 Morel, J. L., Boittin, F. X., Halet, G., Arnaudeau, S., Mironneau, C. and Mironneau, J. (1997) Effect of a 14-day hindlimb suspension on cytosolic  $\text{Ca}^{2+}$  concentration in rat portal vein myocytes. *Am. J. Physiol.* **273**, H2867–H2875
- 16 Tovey, S. C., Godfrey, R. E., Hughes, P. J., Mezna, M., Minchin, S. D., Mikoshiba, K. and Michelangeli, F. (1997) Identification and characterization of inositol 1,4,5-trisphosphate receptors in rat testis. *Cell Calcium* **21**, 311–309
- 17 Neylon, C. B., Richards, S. M., Larsen, M. A., Agrotis, A. and Bobik, A. (1995) Multiple types of ryanodine receptor/ $\text{Ca}^{2+}$  release channels are expressed in vascular smooth muscle. *Biochem. Biophys. Res. Commun.* **215**, 814–821
- 18 Viard, P., Exner, T., Maier, U., Mironneau, J., Nürnberg, B. and Macrez, N. (1999)  $G\beta\gamma$  dimers stimulate vascular L-type  $\text{Ca}^{2+}$  channels via phosphoinositide 3-kinase. *FASEB J.* **13**, 685–694
- 19 De Smedt, H., Missiaen, L., Parys, J. B., Henning, R. H., Sienaert, I., Vanlingen, S., Gijssens, A., Himpens, B. and Casteels, R. (1997) Isoform diversity of the inositol trisphosphate receptor in cell types of mouse origin. *Biochem. J.* **322**, 575–583
- 20 Sun, X. P., Callamaras, N., Marchant, J. S. and Parker, I. (1998) A continuum of  $\text{InsP}_3$ -mediated elementary  $\text{Ca}^{2+}$  signalling events in *Xenopus* oocytes. *J. Physiol. (London)* **509**, 67–80
- 21 Cheng, H., Lederer, M. R., Lederer, W. J. and Cannell, M. B. (1996) Calcium sparks and  $[\text{Ca}^{2+}]_i$  waves in cardiac myocytes. *Am. J. Physiol.* **270**, C148–C159
- 22 Missiaen, L., Taylor, C. W. and Berridge, M. J. (1991) Spontaneous calcium release from inositol trisphosphate-sensitive calcium stores. *Nature (London)* **352**, 241–244
- 23 Bootman, M. D., Berridge, M. J. and Lipp, P. (1997) Cooking with calcium: the recipes for composing global signals from elementary events. *Cell* **91**, 367–373
- 24 Boittin, F. X., Macrez, N., Halet, G. and Mironneau, J. (1999) Norepinephrine-induced  $\text{Ca}^{2+}$  waves depend on  $\text{InsP}_3$  and ryanodine receptor activation in vascular myocytes. *Am. J. Physiol.* **277**, C139–C151
- 25 Sonnleitner, A., Conti, A., Bertocchini, F., Schindler, H. and Sorrentino, V. (1998) Functional properties of the ryanodine receptor type 3 (RyR3)  $\text{Ca}^{2+}$  release channel. *EMBO J.* **17**, 2790–2798
- 26 Thomas, D., Lipp, P., Berridge, M. J. and Bootman, M. D. (1998) Hormone-evoked elementary  $\text{Ca}^{2+}$  signals are not stereotypic, but reflect activation of different size channel clusters and variable recruitment of channels within a cluster. *J. Biol. Chem.* **273**, 27130–27136
- 27 Cardy, T. J., Traynor, D. and Taylor, C. W. (1997) Differential regulation of types-1 and -3 inositol trisphosphate receptors by cytosolic  $\text{Ca}^{2+}$ . *Biochem. J.* **328**, 785–793
- 28 Hagar, R. E., Burgstahler, A. D., Nathanson, M. H. and Ehrlich, B. E. (1998) Type III  $\text{InsP}_3$  receptor channel stays open in the presence of increased calcium. *Nature (London)* **396**, 81–84
- 29 Missiaen, L., De Smedt, H., Droogmans, G. and Casteels, R. (1992) Luminal  $\text{Ca}^{2+}$  controls the activation of the inositol 1,4,5-trisphosphate receptor by cytosolic  $\text{Ca}^{2+}$ . *J. Biol. Chem.* **267**, 22961–22916
- 30 Miyakawa, T., Maeda, A., Yamazawa, T., Hirose, K., Kurosaki, T. and Iino, M. (1999) Encoding of  $\text{Ca}^{2+}$  signals by differential expression of  $\text{IP}_3$  receptor subtypes. *EMBO J.* **18**, 1303–1308
- 31 Callamaras, N., Marchant, J. S., Sun, X. P. and Parker, I. (1998) Activation and coordination of  $\text{InsP}_3$ -mediated elementary  $\text{Ca}^{2+}$  events during global  $\text{Ca}^{2+}$  signals in *Xenopus* oocytes. *J. Physiol. (London)* **509**, 81–91
- 32 Iino, M., Yamazawa, T., Miyashita, Y., Endo, M. and Kasai, H. (1993) Critical intracellular  $\text{Ca}^{2+}$  concentration for all-or-none  $\text{Ca}^{2+}$  spiking in single smooth muscle cells. *EMBO J.* **12**, 5287–5291
- 33 Golovina, V. A. and Blaustein, M. P. (1997) Spatially and functionally distinct  $\text{Ca}^{2+}$  stores in sarcoplasmic and endoplasmic reticulum. *Science* **275**, 1643–1648

Received 18 October 1999/23 March 2000; accepted 14 April 2000